Error analysis and optimal design of reduction relay lens for field of view stitching applications

Xinjie Zhang
School of Mechanical and Aerospace Engineering, Jilin University, Changchun, China and
Changchun Institute of Optics Fine Mechanics and Physics Chinese Academy of Sciences, Changchun, China
Fansen Kong
School of Mechanical and Aerospace Engineering, Jilin University, Changchun, China, and
Zhiyuan Gu and Xiao Shen
Changchun Institute of Optics Fine Mechanics and Physics Chinese Academy of Sciences, Changchun, China

Abstract

Purpose – FOV splicing optical remote sensing instruments have a strict requirement for the focal length consistency of the lens. In conventional optical-mechanical structure design, each optical element is equally distributed with high accuracy and everyone must have a high machining and assembly accuracy. For optical remote sensors with a large number of optical elements, this design brings great difficulties to lens manufacture and alignment.

Design/methodology/approach – Taking the relay lens in an optical remote sensing instrument with the field of view splicing as an example, errors of the system are redistributed to optical elements. Two optical elements, which have the greatest influence on modulation transfer function (MTF) of the system are mounted with high accuracy centering and the other elements are fixed by gland ring with common machining accuracy. The reduction ratio consistency difference among lenses is compensated by adjusting the optical spacing between the two elements.

Findings – Based on optical system simulation analysis, the optimized structure can compensate for the difference of reduction ratio among lens by grinding the washer thickness in the range of ±0.37 mm. The test data for the image quality of the lens show that the MTF value declined 0.043 within ±0.4 mm of space change between two barrels. The results indicate that the reduction ratio can be corrected by adjusting the washer thickness and the image quality will not obviously decline.

Originality/value – This paper confirms that this work is original and has not been published elsewhere nor is it currently under consideration for publication elsewhere. In this paper, the optimum structural design of the reduction relay lens for the field of view stitching applications is reported. The method of adjusting washer thickness is applied to compensate for the reduction ratio consistency difference of lenses. The optimized structure also greatly reduces the difficulty of lenses manufacture, alignment and improves the efficiency of assembly.

Keywords Field-of-view splicing, Optical remote sensor, Optical-mechanical structure design, Reduction ratio consistency

Paper type Technical paper

1. Introduction

Optical remote sensors are widely used in earth observation, deep-space exploration, astronomical observation and military detection and other fields (Hu and Jin, 2017).

Space optical remote sensors with wide field and high resolution are demanded to meet the higher resolution and increasing accuracy requirements in scientific exploration. To solve this problem, inner stitching, also known as image square stitching, is applied in some optical remote sensors to achieve higher resolution and a wider field of view (Zhang and Gao, 2018; Jiang *et al.*, 2015; Zhang *et al.*, 2014). For example, the high-resolution cameras carried by Quick Bird, IKONOS, ZY-102C and TH-1 satellites mounted multiple TDI CCDs on a focal plane into up-and-down staggered double columns and an image of each detector is seamlessly stitched to achieve higher resolution. Also, there are some optical remote sensors using external splicing to align, which multiple fields with independent optical systems and detectors. Some satellites such as BJ-1, ZY-1 02 C, GF-1, high GF-2 adopted multi-lens external stitching (Wang *et al.*, 2014; Zhang *et al.*, 2015; Zheng and Zhang, 2016)

For both internal and external stitching, a highly precise and seamless stitching image registration is vital to ensure image accuracy and stability Wang *et al.*, 2014; Cheng *et al.*, 2015. Therefore, both of the methods require optical and mechanical structures with high accuracy manufacture and alignment. To improve the efficiency of manufacture and alignment stitching lenses, several studies have been conducted on structure design and alignment of the optical system. Z.J. Liu proposed an optical alignment method of the coaxial optical system based on the global optimization alignment method. The optimization model was established by fitting the surface error of part. This method can compensate for the optical centering

The current issue and full text archive of this journal is available on Emerald Insight at: **https://www.emerald.com/insight/0260-2288.htm**

Sensor Review
41/1 (2021) 87–92
© Emerald Publishing Limited [ISSN 0260-2288]
[DOI 10.1108/SR-03-2020-0070]

Received 23 March 2020
Revised 3 December 2020
Accepted 20 December 2020

errors very well but cannot compensate for the reduction ratio consistency difference among lenses (Liu and Yi, 2017). L Jiang introduced a high zoom-ration zoom optical system. In this system, two lenses were used to compensate for the temperature error, but not introduced how to select the lens for temperature compensation (Jiang and Huang, 2011). J Li introduced a nonuniformity correction method based on radiation calibration, which can be used in a three-lens polarizing CCD camera. This method was to correct the nonuniformity through processing the polarization data of the original image but cannot compensate for non-uniformity during the assembly process (Li and Yi, 2011).

To reduce the manufacture and alignment difficulty and compensate for the reduction ratio consistency difference among lenses during the assembly process, a relay lens of an optical remote sensor using external stitching is taken as an example to distribute the error of the optical system of the lens. Two optical elements with the largest influence on the Modulation Transfer Function (MTF) are selected to centering aligned and the spacing between the two elements is aligned to compensate for the reduction ratio consistency difference of lenses. The optical simulation analysis results and the test data of MTF indicate the method could meet the requirements of optical performance.

2. Design of optical-mechanical structure

2.1 Optical system design

The task of the relay lens of the optical remote sensing instrument is to realize the zoom imaging in visible and near-infrared channels. There are 27 relay lenses in the optical remote sensing instrument for the field of view splicing. The lenses are placed in two stagger rows. The optical system of the relay lens consists of nine optical elements. The optical system is shown in Figure 1. The optical parameters are shown in Table 1.

Some parameter requirements for the optical system are shown in Table 2.

The relay lenses are required to be simple in structure, easy to install and adjust, replace, light in weight, adapt to the space environment and meet the mechanical requirements.

2.2 Error analysis

To ensure the alignment accuracy, the optical system of space optical remote sensing instrument with the field of view splicing generally has each optical element aligned in the independent mount and centered thru high precision centering lathe. The lens holder is assembled into the barrel, in turn (Zhang *et al.*, 2018; Guo *et al.*,2012; Li, 2016; Dong, 2012; Zhang and Lv, 2015).

Figure 1 The optical system of relay lenses

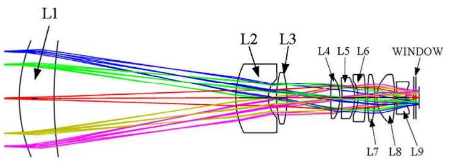

Table 1 Optical parameters

No.	Material	Radius/mm	Thickness/mm	Aperture/mm
L1	N-LAK34	34.90	8.00	34
		95.69	41.83	
L2	N-SF8	18.45	7.50	16.00
		6.36	1.90	
L3	LF5	24.23	2.40	12.00
		−23.62	10.06	
L4	N-FK51A	78.30	2.10	9.6
		−9.40	0.50	
L5	N-LAK14	−45.29	2.90	9.6
		−10.77	0.79	
L6	N-SF8	−7.71	1.70	11.0
		−49.00	0.50	
L7	N-LAK14	46.30	1.65	11.0
		−23.89	0.50	
L8	N-PSK53A	7.56	4.10	11.0
		−30.64	0.50	
L9	N-SF8	−40.29	2.10	7.6
		6.84	1.77	
WINDOW	SAPPHIRE	Infinity	0.50	11
		Infinity	0.75	

Table 2 Optical technical requirements for the relay lens

Optical parameters	Target
Field	28mm × 22mm
Reduction ratio	1:7
Reduction ratio consistency	±0.05%

Referring to the machining accuracy of centering installation, the optical element alignment error of centering installation is shown in Table 3.

We know that the refractive index of the glass is 1/1,000, Abbe's value is 0.5%, surface irregularity is ±0.2 fringes, According to the tolerance value in Table 3, the tolerances of nine elements are brought into the optical system of the reduction relay lens in Zemax OpticStudio. The MTF at 20 lp/mm is used as the criterion for tolerancing. The results of the MTF analysis of the relay lens obtained by the Monte Carlo method with 500 samples are shown in Table 4.

Table 4 shows that 98% of samples have a decrease of less than 0.038 in MTF@201p/mm. The imaging quality can meet the imaging requirements.

Table 3 Installation tolerance for optical elements

Tolerance	Value
Radius of curvature	±1 fringes
Thickness	±0.02 mm
Decenter of element	±0.01 mm
Tilt of element	±0.1°

Table 4 MTF for centering element

Probability (%)	Average MTF @ 20 lp/mm
98	≥0.793
90	≥0.812
80	≥0.820
50	≥0.832
20	≥0.844
10	≥0.848

2.3 Structural design

According to the above error analysis, the optical and mechanical structure design of the relay lens was carried out. The element is centering fixed by rolling edge because the diameter of the element is small. The installation method is shown in Figure 2. The inner diameter of the lens holder is matched with the outer diameter of the optical element to ensure that the radial clearance between the element and the lens holder is less than +0.05 mm. The lens holder with element is clamped on a high precision centering lathe. The measuring system aims at the optical axis of the lens, adjust the revolving axis of the lathe's centering clamp to coincide with the optical axis. The outer diameter and upper and lower sections of the lens holder are processed to complete the centralized assembly of one lens.

Then the one lens holder with optical element is mounted into the lens barrel, in turn, and aligned with a centralizer to complete the assembly of the whole lens, as shown in Figure 3.

3. Optimal design

From the analysis above, it can be seen that the method of installing each optical element independently and centrally has high accuracy, stability and reliability and is suitable for the optical sensor with fewer lenses. However, as this method requires separate centering and mounting of each optical element, the manufacture and installation efficiency of the lens is greatly reduced. This method is obviously time-consuming and laborious for a lens with more optical elements or optical remote sensor with many lenses. So when it comes to the sensor with 27 relay lenses, each of which contains nine optical elements, the method is not suitable. To improve the efficiency of manufacture and adjustment, we optimize the structure of the lens.

Figure 2 Diagram of lens centering installation

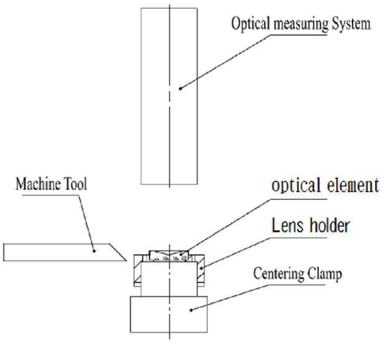

Figure 3 Diagram of lens centering

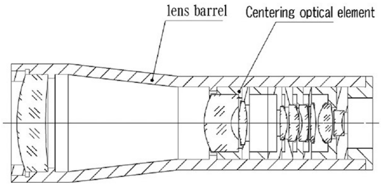

3.1 Error optimization

We use Zemax OpticStudio to analyze the decenter and tilt error of the optical elements in the sensitivity analysis of optical tolerance. The sensitivity of the decenter error and tilt error of each optical element to the MTF value can be obtained. Then the decenter sensitivity D (i) of the element is defined to indicate the MTF decrease caused by the decenter error of 0.01 mm of the i-th element; the tilt sensitivity T (i) of the element indicates the MTF decrease caused by the tilt error of 0.1° of the i-th element; the specific values are shown in Table 5.

To determine the influence of decentering and tilt error on the MTF value of the optical system, the misalignment sensitivity coefficient MS (i) of the element is defined, as shown in the formula (1).

$$MS(i) = \sqrt{T(i)^2 + D(i)^2} \tag{1}$$

The misalignment sensitivity of each element is calculated as shown in Table 6.

Table 5 Sensitivity for element

Element no.	Decenter sensitivity (D)	Tilt sensitivity (T)
L1	0.00001	0.00001
L2	0.00154	0.01295
L3	0.00005	0.00012
L4	0.00221	0.00112
L5	0.00183	0.00073
L6	0.00418	0.00385
L7	0.00020	0.00015
L8	0.00030	0.00060
L9	0.00034	0.00077

Table 6 MS sensitivity of the element

Element no.	Misalignment sensitivity (MS)
L1	0.00001
L2	0.01304
L3	0.00013
L4	0.00248
L5	0.00197
L6	0.00568
L7	0.00025
L8	0.00067
L9	0.00085

It can be seen from the data that the tolerances of element 2 and element 6 have a great influence on the imaging quality. Therefore, the errors of the lens are redistributed. Element 2 and element 6 are mounted by centering and the other elements are fixed by ring pressing which the assembly errors are guaranteed by the accuracy of common mechanical processing.

3.2 Structure design for reduction ratio consistency compensation

The consistency of the reduction ratio of 27 lenses in the optical remoter sensor is required less than 0.05%. The traditional method is to ensure high precision by improving the accuracy of manufacture and adjusting, which is difficult to achieve by ordinary machine tools. To reduce the difficulty of manufacture, it is possible to produce parts in large quantities and select the parts that meet the requirements to align the lenses. This method is time-consuming, labor-consuming and extremely inefficient. To improve the efficiency and to meet the requirements of the consistency of the reduction ratio, we propose a method that the consistency of the reduction ratio is compensated through adjusting the optical spacing between two elements.

By taking the axial distance between two elements of the lens as compensation, the consistency of the reduction ratio is ensured by adjusting the compensation. The back focal length is adjusted to guarantee a focal plane focus. The selection of the reduction ratio compensator should in principle be that the change of the compensator has little effect on the image quality and it is moderately sensitive to the reduction ratio. Because the high sensitivity will increase the compensation accuracy requirement and the sensitivity is too low, which may result in excessive compensation

Through the optical analysis, the compensation of the reduction ratio between the two elements spacer is shown in Table 7.

From the above table, it can be seen that the distance compensation range of element 1 and element 2 is moderate (+0.37 mm) and the accuracy of spacing adjustment is low (17 μm). In the optical structure, the optical spacing between element 1 and element 2 is large and easy to adjust. Therefore, the optical spacing of element 1 and element 2 is selected as the compensation of reduction ratio.

Table 7 Compensation range and accuracy requirement for spacing

Spacing	Compensation range (mm)	Compensation accuracy requirement (μm)
L1-L2	±0.37	17
L2-L3	±0.1	5
L3-L4	±0.28	13
L4-L5	±0.24	11
L5-L6	±3.58	161
L6-L7	±0.33	15
L7-L8	±0.49	23
L8-L9	±0.04	2

3.3 Structural optimization

According to the above analysis, it is obvious that the tolerances of element 2 and element 6 have the greatest influence on the imaging quality of the optical system. To ensure the imaging quality of the optical system, element 2 and element 6 are mounted by centering. The rest elements are fixed by ring pressing and spacers to ensure assembly precision by machining accuracy.

Through the analysis of optical parameters, the optical spacing between element 1 and element 2 is more sensitive to the change of reduction ratio. By adjusting the optical spacing between element 1 and element 2, the consistency difference of reduction ratio between lenses can be compensated.

Therefore, the element from 2 to 9 are integrated into barrel 2. The washer of 1.5 mm thickness is placed between barrel 1 and barrel 2 and the reduction ratio is measured during the assembly and imaging test process. The optical spacing difference between element 1 and element 2 is determined in accordance with the reduction ratio difference between the lenses. Eventually, the thickness of the washer of each element is calibrated on the basis of the calculated value so as to achieve satisfaction with reduction ratio consistency. The optimized model is established by UG. The detailed structure is shown in Figure 4. The structural material of the lens is the aluminum alloy.

4. Simulation analysis

Optical simulation of the optimized structure design is carried out. According to Figure 4, the errors of the optical elements are shown in Table 8 below.

Based on the tolerance values above, the tolerance results are analyzed by the Monte Carlo method with 500 samples, and the optimized lens MTF is shown in Table 9.

As shown in the table above, the decrease of MTF@20lp/mm in 98% of the samples in this design method is less than 0.08 and the imaging quality can also meet the imaging quality requirements. Figure 5. is the comparison between MTF before

Figure 4 Optimized structural diagram

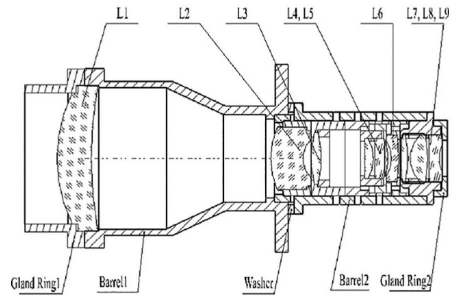

Table 8 Installation tolerance for elements

Tolerance	Element 2 and element 6	Other elements
Radius of curvature	±1 fringes	±1 fringes
Thickness	±0.02 mm	±0.02 mm
Decenter of element	±0.01 mm	±0.02 mm
Tilt of element	±0.1°	±0.2°

Table 9 MTF for optimized camera

Probability (%)	AverageMTF@20lp/mm
98	≥0.751
90	≥0.777
80	≥0.789
50	≥0.811
20	≥0.825
10	≥0.829

Figure 5 MTF comparison before and after optimization

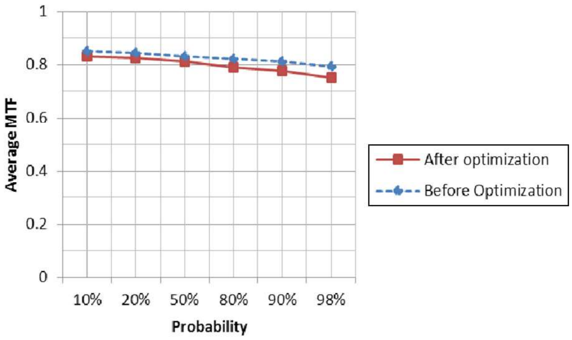

and after optimization. It can be seen from Figure 5 that the MTF slightly decreased and the analysis results also meet the image quality requirements.

The analysis of the optical system indicates that the difference in the reduction ratio can be compensated by adjusting the optical spacing between element 1 and element2 within ± 0.37 mm. When the thickness of the washer between element 1 and element 2 is adjusted within ± 0.37 mm, the MTF of the lens analyzed by the Monte-Carlo method is shown in Table 10.

The simulation results show that by adjusting the washer between element 1 and element 2, the difference in reduction ratio can be well compensated and the image quality of the lens will not be greatly affected.

5. Experimental

The image quality of the optimized lens was tested by measuring its MTF. The optimized structure of the lens was shown in Figure 6.

The thickness change of the washer was carried out by adjusting the space between barrel1 and barrel2. MTF of the lens in different spaces was measured by optical transmission function (OTF) tester just as Figure 7 showed.

Table 10 MTF of the lens after adjusting the thickness of washer

	+0.37mm	−0.37mm
98%	0.736	0.721
90%	0.767	0.75
80%	0.780	0.763
50%	0.797	0.781
20%	0.809	0.797
10%	0.814	0.804

Figure 6 Optimized structure of the lens

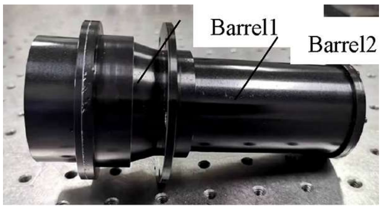

The space between barrels was adjusted by an optical bench adjusting bracket. It was known that the theoretical space is 1.5 mm. Due to some factors induced by the machining and fitting process, the real best image quality was at 1.4 mm space of barrels. MTF values were measured every 0.1 mm gap. The test data of MTF are shown in Table 11.

The comparison of optical simulation and test data is shown in Figure 8.

Figure 7 MTF measurement

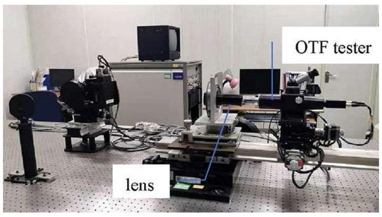

Table 11 Test data of MTF

Space (mm)	MTF
1.0	0.706
1.1	0.723
1.2	0.736
1.3	0.745
1.4	0.749
1.5	0.746
1.6	0.739
1.7	0.728
1.8	0.715

Figure 8 Test data of MTF

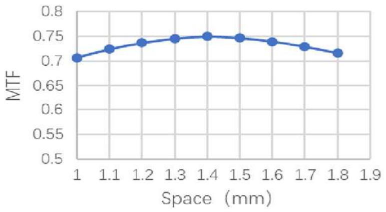

From Table 11, it can be seen that the MTF value declined 0.043 within ± 0.4 mm of space change between barrel1 and barrel 2. The results are consistent with the simulation results, which show that the image quality will not obviously decline with adjusting the washer thickness.

6. Conclusion

To improve the efficiency of manufacture and installation of field-of-view splicing lenses, we present a new approach to redistribute the lens error among the lenses of the remote sensor and optimize the installation structure of the lens. Two optical elements, which have the greatest influence on MTF of the system are mounted with high accuracy centering and the other elements are fixed by gland ring with common machining accuracy. By adjusting the thickness of the washer between two elements to adjust the reduction ratio, the requirement of reduction ratio consistency among lenses can be satisfied. Optical simulation analysis results show that the optimized structure can compensate for the difference of reduction ratio among lens by grinding the washer thickness in the range of ± 0.37 mm, which can meet the requirements of 0.05% reduction ratio consistency and imaging quality. The test data of MTF indicated that the image quality of the lens was not obviously declined through changing spacer between the two barrels. The test results were in accordance with optical simulation. The optimized structure greatly reduces the difficulty of lens processing and adjustment and greatly improves the installation efficiency of the lens.

References

Cheng, Y.F., Jin, S.Y., Wang, M., *et al.* (2017), “An high accuracy image mosaicking approach of optical remote sensing satellite for muti-camera system”, *ACTA Optical SINICA*, Vol. 37 No. 8, 0828003-1-0828003-8.

Dong, S.H. (2012), *Optical Centering Processing and Assembly Technology Research*, Changchun University of Science and Technology.

Guo, X.R., Liao, Z.B., Wang, C.H.Y., *et al.* (2012), “Aberration and alignment quality investigation of space transmission optical system with centering error of optical axes”, *Infrared and Laser Engineering*, Vol. 41 No. 2, pp. 436-441.

Hu, F. and Jin, S.Y. (2017), “Study on the development of wide swath imaging technology about high resolution optical remote sensing satellites”, *Geomatics World*, Vol. 24 No. 5, pp. 45-50.

Jiang, L. and Huang, W. (2011), “Lens design for optical system of high zoom ratio”, *ACTA Optical Sinica*, Vol. 12 No. 31, pp. 1222006-1.

Jiang, Y.H., Zhang, G., Li, D.R., *et al.* (2015), “Correction of distortions in YG-12 high-resolution panchromatic images”, *Photogrammetric Engineering & Remote Sensing*, Vol. 81 No. 1.

Li, X.H. (2016), “Research on the structure of multiband shared aperture imaging system based on the consistency of the fields of view”, Changchun Institute of Optics, Fine Mechanics and Physics, Chinese Academy of Sciences.

Li, J. and Yi, W.N. (2011), “Nonuniformity correction of a three-lens polarizing CCD camera”, *Infrared*, Vol. 4 No. 32, pp. 15-34.

Liu, Z.J. and Yi, G.W. (2017), *The Assembly Accuracy Analysis and Alignment Optimization of Coaxial Optical System*, Hunan University.

Wang, M., Yang, B., Hu, F., *et al.* (2014), “On-orbit geometric calibration model and its applications for high-resolution optical satellite imagery”, *Remote Sensing of Sensing*, Vol. 6 No. 5.

Wang, M., Song, L.W. Qiao, Y.F., *et al.* (2010), “External field stitching technology for high speed target measuring and its implementation”, *Opto Precision Engineering*, Vol. 9 No. 18, pp. 2069-2076.

Zhang, X. and Gao, Y.G. (2018), “Large field of view imaging system for remote target capture and trajectory measurement based on cone rotation”, *Review of Scientific Instruments*, Vol. 89 No. 6, p. 063704, available at: https://doi.org/10.1063/1.5023757

Zhang, L.M. and Lv, T.Y. (2015), “Research for fixing and orientation structure of lens”, *Laser & Optoelectronics Progress*, Vol. 52, pp. 042202-1-042202-6.s.

Zhang, X., Gao, Y.G., Xue, X.Y., *et al.* (2018), “Large field-of-view stitching with a single lens and its implementation”, *Optics and Precision Engineering*, Vol. 26 No. 6, pp. 1346-1353.

Zhang, Y.J., Zheng, M.T., Xiong, J.X., *et al.* (2014), “On-orbit geometric calibration of ZY-3 three-line array imagery with multistrip data sets”, *IEEE Transactions on Geoscience and Remote Sensing*, Vol. 52 No. 1.

Zhang, Y.J., Zheng, M.T., Xiong, X.D. *et al.* (2015), “Multistrip bundle block adjustment of ZY-3 satellite imagery by rigorous sensor model without ground control point”, *Geoscience and Remote Sensing Letters IEEE*, Vol. 12 No. 4, pp. 865-869.

Zheng, M.T. and Zhang, Y.J. (2016), “DEM-Aided bundle adjustment with multisource satellite imagery: ZY-3 and GF-1 in large areas”, *IEEE Geoscience and Remote Sensing Letters*, Vol. 13 No. 6, pp. 880-884.

Corresponding author

Fansen Kong can be contacted at: kongfs@jlu.edu.cn